

The fate of the $2\sqrt{3} \times 2\sqrt{3}R(30^\circ)$ silicene phase on Ag(111)

Zhi-Long Liu, Mei-Xiao Wang, Canhua Liu, Jin-Feng Jia, Patrick Vogt, Claudio Quaresima, Carlo Ottaviani, Bruno Olivieri, Paola De Padova, and Guy Le Lay

Citation: *APL Materials* **2**, 092513 (2014); doi: 10.1063/1.4894871

View online: <https://doi.org/10.1063/1.4894871>

View Table of Contents: <http://aip.scitation.org/toc/apm/2/9>

Published by the [American Institute of Physics](#)

Articles you may be interested in

[Epitaxial growth of a silicene sheet](#)

Applied Physics Letters **97**, 223109 (2010); 10.1063/1.3524215

[The instability of silicene on Ag\(111\)](#)

Applied Physics Letters **103**, 263119 (2013); 10.1063/1.4860964

[Evidence of Dirac fermions in multilayer silicene](#)

Applied Physics Letters **102**, 163106 (2013); 10.1063/1.4802782

[Silicene: Recent theoretical advances](#)

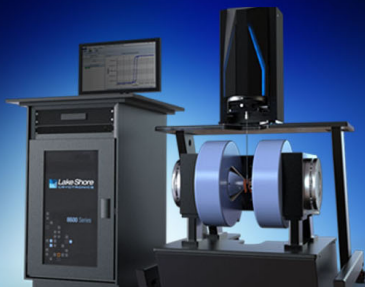
Applied Physics Reviews **3**, 040802 (2016); 10.1063/1.4944631

[Synthesis and electrical conductivity of multilayer silicene](#)

Applied Physics Letters **104**, 021602 (2014); 10.1063/1.4861857

[Evidence for hybrid surface metallic band in \$\(4 \times 4\)\$ silicene on Ag\(111\)](#)

Applied Physics Letters **103**, 231604 (2013); 10.1063/1.4841335



NEW 8600 Series VSM

For fast, highly sensitive
measurement performance

LEARN MORE 

The fate of the $2\sqrt{3} \times 2\sqrt{3}R(30^\circ)$ silicene phase on Ag(111)

Zhi-Long Liu,^{1,2} Mei-Xiao Wang,^{1,2} Canhua Liu,^{1,2,a} Jin-Feng Jia,^{1,2}
 Patrick Vogt,³ Claudio Quaresima,⁴ Carlo Ottaviani,⁴ Bruno Olivieri,⁵
 Paola De Padova,^{4,a} and Guy Le Lay^{6,a}

¹Key Laboratory of Artificial Structures and Quantum Control (Ministry of Education),
 Department of Physics and Astronomy, Shanghai Jiao Tong University, Shanghai 200240,
 People's Republic of China

²Collaborative Innovation Center of Advanced Microstructures, Nanjing 210093,
 People's Republic of China

³Technische Universität Berlin, Institut für Festkörperphysik, Hardenbergstraße 36,
 10623 Berlin, Germany

⁴CNR-ISM, via Fosso del Cavaliere, Rome 00133, Italy

⁵ISAC-CNR, via Fosso del Cavaliere 100, Rome, Italy

⁶Aix-Marseille Université, CNRS, PIIM UMR 7345, 13397, Marseille, France

(Received 1 July 2014; accepted 27 August 2014; published online 8 September 2014)

Silicon atoms deposited on Ag(111) produce various single layer silicene sheets with different buckling patterns and periodicities. Low temperature scanning tunneling microscopy reveals that one of the silicene sheets, the hypothetical $\sqrt{7} \times \sqrt{7}$ silicene structure, on $2\sqrt{3} \times 2\sqrt{3}$ Ag(111), is inherently highly defective and displays no long-range order. Moreover, Auger and photoelectron spectroscopy measurements reveal its sudden death, to end, in a dynamic fating process at $\sim 300^\circ\text{C}$. This result clarifies the real nature of the $2\sqrt{3} \times 2\sqrt{3}R(30^\circ)$ silicene phase and thus helps to understand the diversity of the silicene sheets grown on Ag(111). © 2014 Author(s). All article content, except where otherwise noted, is licensed under a Creative Commons Attribution 3.0 Unported License. [<http://dx.doi.org/10.1063/1.4894871>]

There is a boom in research on silicene,¹ graphene's silicon based cousin, that is, a monolayer of silicon atoms arranged in a buckled two-dimensional (2D) honeycomb lattice,² since its first artificial creation on silver (111)^{3,4} and zirconium (0001) templates.⁵ Indeed, this boom is related to the fact that silicene is expected to share the same exotic properties as graphene, and, hence, be similarly a new wonder material, with the advantage of being more easily compatible with the current electronics industry.

Single layer silicene grown on Ag(111), presently the favored substrate, can form various atomic structures with different buckling patterns and periodicities,⁶ however, two main ordered phases dominate. The first one is a 3×3 reconstructed silicene sheet coinciding with a 4×4 Ag(111) supercell, hereafter named $3 \times 3/4 \times 4$, which is synthesized at $\sim 220^\circ\text{C}$ and forms a beautiful "flower pattern" in scanning tunneling microscopy (STM) imaging (see Fig. 1(a)),³ while possibly covering 95% of the total silver single crystal surface area.⁷ Its nominal coverage ratio in Si atoms, θ_{Si} is $18/16 = 1.125$ and the in-plane Si-Si nearest neighbor distance $d_{\text{Si-Si}}$ is 0.225 nm, comparable to the calculated value for free standing silicene of 0.21 nm.² The second one is a $\sqrt{7} \times \sqrt{7}R(\pm 19.1^\circ)$ reconstructed silicene sheet coinciding with a $\sqrt{13} \times \sqrt{13}R(\pm 13.9^\circ)$ Ag(111) supercell, hereafter named $\sqrt{7} \times \sqrt{7}/\sqrt{13} \times \sqrt{13}$, synthesized at temperatures between 220°C and 250°C , with slightly lower nominal coverage of $14/13 = 1.08$ and slightly expanded $d_{\text{Si-Si}}$ of 0.23 nm [see Fig. 1(d)].^{8,9} Indeed, symmetry imposes four equivalent domains for the $\sqrt{7} \times \sqrt{7}/\sqrt{13} \times \sqrt{13}$ on the Ag(111) surface, which have been simultaneously observed on a single STM image.¹⁰ However, under these preparation conditions both $3 \times 3/4 \times 4$ and $\sqrt{7} \times \sqrt{7}/\sqrt{13} \times \sqrt{13}$ phases co-exist.¹¹

^aElectronic addresses: canhualiu@sjtu.edu.cn; depadova@ism.cnr.it; and guy.lelay@univ-amu.fr

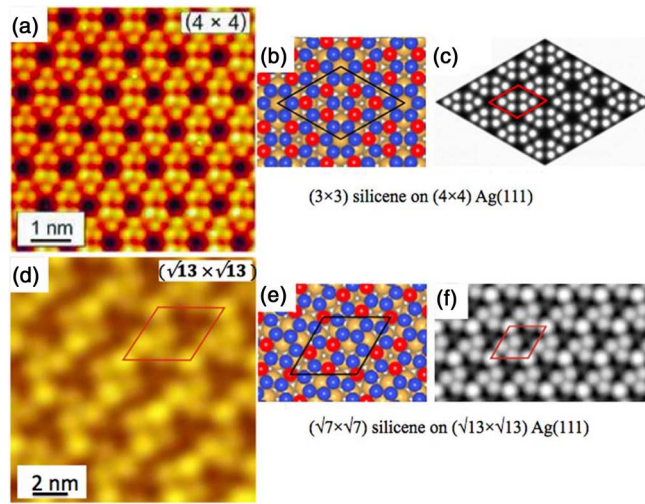


FIG. 1. The main $3 \times 3/4 \times 4$ and $\sqrt{7} \times \sqrt{7}/\sqrt{13} \times \sqrt{13}$ phases of single layer silicene grown on the Ag(111) surface. (a) High-resolution STM image ($6 \times 6 \text{ nm}^2$, $U_{\text{bias}} = -1.12 \text{ V}$, $I = 0.65 \text{ nA}$) of the $3 \times 3/4 \times 4$ silicene monolayer phase acquired under UHV conditions ($< 2 \times 10^{-10}$ Torr); the “flower-pattern” that results from the upward displacement of 6 of the 18 Si atoms in the honeycomb structure is clearly visible. (d) STM image (UHV, $4 \times 4 \text{ nm}^2$, $U_{\text{bias}} = 0.10 \text{ V}$, $I = 0.1 \text{ nA}$) of $\sqrt{7} \times \sqrt{7}/\sqrt{13} \times \sqrt{13}$ silicene. (b) and (e) Models of the two ideal structures and corresponding calculated STM images (c) and (f) (after Fig. 8 of Ref. 9 and Fig. 11 of Ref. 12).

When Si is deposited onto the Ag(111) surface at higher temperatures, typically $> 250^\circ \text{C}$, STM images with a highly defective appearance are observed at room temperature; accompanying (rather poor) low energy electron diffraction (LEED) patterns of a “quasi-pure” $2\sqrt{3} \times 2\sqrt{3}R(30^\circ)$ at 300°C led Jamgotchian *et al.* to assign this to a new “ $2\sqrt{3} \times 2\sqrt{3}R(30^\circ)$ silicene phase” in terms of the silver coincidence supercell.¹³ Ideally, if really existing, this phase would correspond to a $\sqrt{7} \times \sqrt{7}R(\pm 19.1^\circ)$ reconstructed silicene sheet, which should be described as $\sqrt{7} \times \sqrt{7}/2\sqrt{3} \times 2\sqrt{3}$, using our labeling. The nominal Si coverage ratio would be 1.17, a bit higher than those of the $3 \times 3/4 \times 4$ and $\sqrt{7} \times \sqrt{7}/\sqrt{13} \times \sqrt{13}$ phases, while the Si–Si in-plane distance would be 0.218 nm, that is, somewhat lower than in the previous cases.

However, as mentioned above, only highly defective STM images have been shown until now,^{13–15} bearing strong similarity with the one we have recorded at low temperature, which is displayed in Fig. 2 along with the inserted image simulated by Guo *et al.*, for a hypothetical ideal $\sqrt{7} \times \sqrt{7}/2\sqrt{3} \times 2\sqrt{3}$ silicene structure on Ag(111).¹⁶ As indicated by the encircled regions, such a configuration does exist, but only just very locally, and, overall, non periodically, in a disordered way.

As a matter of fact, the assignment to a $2\sqrt{3} \times 2\sqrt{3}R(30^\circ)$ superstructure with respect to the silver substrate surface has been questioned:¹⁷ such a superstructure was not observed by Arafune *et al.*, in a thorough detailed LEED and STM study.⁸ We note in passing that a highly perfect, “ $2\sqrt{3} \times 2\sqrt{3}R(30^\circ)$ silicene phase,” prematurely claimed to have been grown essentially without any defect between 220 and 250°C ,^{18,19} has been proved to be just a delusive phase, i.e., a contrast reversed appearance of the bare Ag(111) surface.^{20,21}

The $2\sqrt{3} \times 2\sqrt{3}R(30^\circ)$ superstructure, as grown by Moras *et al.* at 296°C (in short, $2\sqrt{3}$ superstructure), shows, at monolayer completion, an abrupt drop of the intensities of its relevant spots measured in LEED and a concomitant strong increase of the silver integer ones in the course of detailed LEED observations, as shown in Fig. 4 of Ref. 17. Correlatively, the intensity of $\sqrt{3} \times \sqrt{3}R(30^\circ)$ reconstructed bi-layer Si islands (note that, as a communality, this reconstruction is no longer referred to silver, but to silicene itself; if referred to silver it would have to be noted as a $4/\sqrt{3} \times 4/\sqrt{3}R(30^\circ)$ superstructure⁸) increases also, which points to a surface dewetting process occurring when the formation of multilayer regions destabilizes the $2\sqrt{3}$ superstructure, as already described by Acun *et al.* in a previous LEEM study.²²

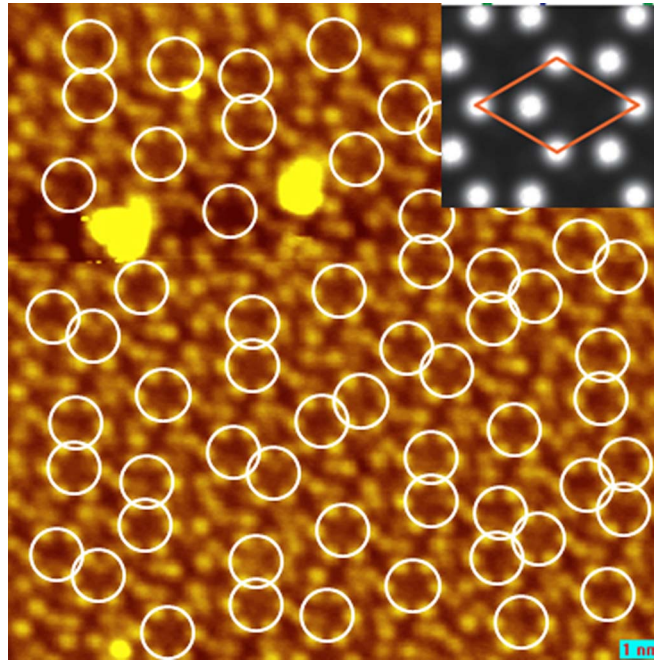


FIG. 2. STM image of the $2\sqrt{3} \times 2\sqrt{3}R(30^\circ)$ superstructure recorded at 77 K ($15 \times 15 \text{ nm}^2$, $U_{\text{bias}} = 95.3 \text{ mV}$, $I = 0.2 \text{ nA}$). The aperiodic circles indicate very local honeycomb arrangements corresponding to the simulated STM image (in inset, after Fig. 2(e) of Ref. 16) of an ideally $2\sqrt{3} \times 2\sqrt{3}R(30^\circ)$ reconstructed silicene sheet.

We have followed this type of evolution using spectroscopy measurement to give a quantitative evaluation of the peculiar behavior. Typically, we plotted the evolution of the relative intensities of characteristic signals (Si LVV/Ag MNN) in Auger electron spectroscopy measurements during growth of the $2\sqrt{3}$ superstructure at 303°C , as shown in Fig. 3 (we have obtained the same trend upon photoelectron spectroscopy measurements shown as an inset at $\sim 300^\circ\text{C}$).

We first stress that the maximum Si LVV/Ag MNN intensity ratio is obtained after a deposition time of ~ 100 min, while it takes just ~ 35 min upon growth at 220°C , using the same impinging flux. This indicates in-diffusion of Si atoms at this too high temperature. Obviously, two kinetic processes compete: the spreading of the $2\sqrt{3}$ superstructure and the incorporation of silicon into the silver sample. Next, we emphasize the sudden drop during growth of the intensity ratio, after ~ 100 min deposition time, which we relate to the dewetting process mentioned above and illustrate in the top left inset.

At this stage we stress that not only the same periodicity points to the uniqueness of this $2\sqrt{3}$ superstructure but also the similar appearance of the STM images, the practically identical growth conditions under which the structure is observed, and, moreover, the same type of fading decay determined in our quantitative AES intensity measurements as the one typically observed in LEED by Moras *et al.*¹⁷ (top left inset in Fig. 3).

The decay of the intensity ratio was followed during ~ 100 additional minutes with the Si cell turned off. Following a rapid drop, the ratio levels off to a small, but non-zero, value, while the $2\sqrt{3}$ -like LEED pattern, as shown in the right down inset of Fig. 3, is still present. This peculiar behavior results again from the competing kinetic processes at stake, namely, dewetting/islanding and in-diffusion. However, we believe that in-diffusion does not go far below the surface; instead, a confined sub-surface alloy yielding the $2\sqrt{3}$ -like LEED pattern, is probably formed, as is, for example, the case of the $c(2 \times 2)$ superstructure formed upon deposition of manganese on a Pd(100) surface.²³

This scenario explains the fading tendency of the $2\sqrt{3}$ superstructure, as expressed by the authors of Ref. 22, and why it appears so highly defective in STM imaging. As a matter of fact it is totally unstable, while in a struggle during growth with the competing formation of the confined sub-surface alloy.

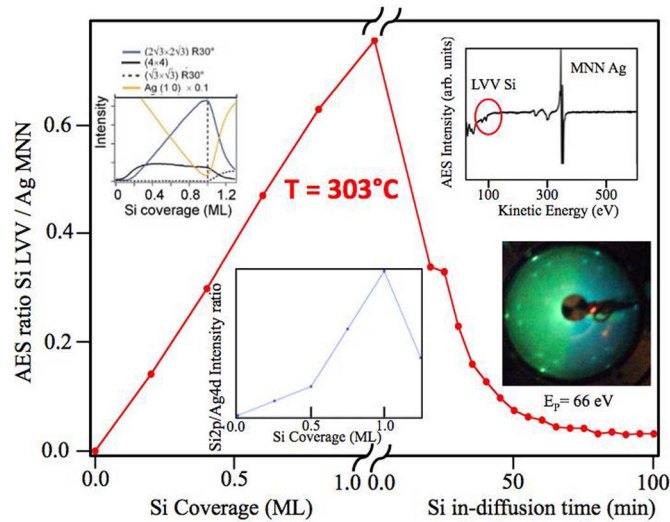


FIG. 3. Relative Auger intensities plotted during growth at 303 °C. A typical Auger spectrum as well as a LEED pattern (taken at 66 eV) after decay are displayed (right insets), along with intensity variations of relevant LEED spots recorded 296 °C (top left inset, after Fig. 4 of Ref. 17). The middle inset shows the evolution of the Si 2p/Ag 4d intensity ratio at ~ 300 °C.

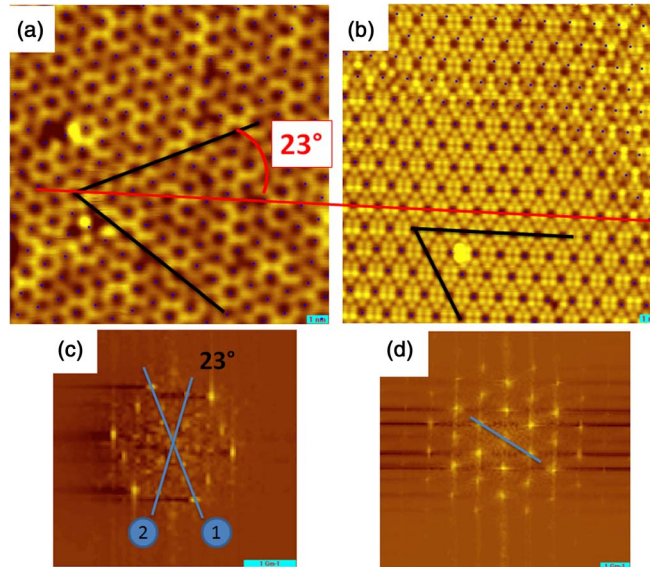


FIG. 4. (a) and (b) Simultaneously acquired STM images of two domains at 4.2 K: the $2\sqrt{3} \times 2\sqrt{3}R(30^\circ)$ superstructure on the left and the $3 \times 3/4 \times 4$ silicene phase on the right with superposed corresponding grids (15 nm \times 15 nm; $U = -2.5$ V, $I = 0.1$ nA). (c) and (d) The respective Fast Fourier transforms of the images in (a) and (b), with markers to determine distances and orientation.

Perusal at STM images taken at 4.2 K, like the ones shown in Fig. 4, helps understanding the defective nature of the $2\sqrt{3}$ superstructure with respect to the reference $3 \times 3/4 \times 4$ silicene phase.

The two STM images displayed in Figs. 4(a) and 4(b) are enlargements of cropped regions from the same high-resolution large scale image comprising several domains. One notices that while the superposed grid nicely matches for the $3 \times 3/4 \times 4$ silicene phase, it deviates markedly for the $2\sqrt{3}$ superstructure. Furthermore, a main orientation of the observed hexagons is at $\sim 23^\circ$ from the $[-110]$ direction of the silver (111) surface, indicated by the red line, instead of 30° , the angle that a true $2\sqrt{3} \times 2\sqrt{3}R(30^\circ)$ superstructure would give. This is confirmed by the respective Fast Fourier transforms shown in Figures 4(c) and 4(d), where the markers point to the correct lattice parameter

$a = 1.157$ nm for the $3 \times 3/4 \times 4$ silicene phase, but, at variance, indicate two co-existing Fourier components at $\sim 23^\circ$ from each other, with periods of 1.012 nm and 1.222 nm, revealing an intimate blend of local $2\sqrt{3} \times 2\sqrt{3}R(30^\circ)$ and, most probably, $\sqrt{19} \times \sqrt{19}R(\pm 23.4^\circ)$ structures. Indeed, in principle, a $\sqrt{19} \times \sqrt{19}R(\pm 23.4^\circ)$ silver superstructure could accommodate a strained, in extension, 3×3 silicene sheet, with a Si–Si distance of 0.242 nm and a Si coverage ratio of 0.95, lower than that of the reference $3 \times 3/4 \times 4$ silicene phase: $\theta_{\text{Si}} = 1.125$. The STM observations indicate that this is possible only very locally. Since, as already mentioned, a $2\sqrt{3} \times 2\sqrt{3}R(30^\circ)$ superstructure could accommodate a $\sqrt{7} \times \sqrt{7}R(\pm 19.1^\circ)$ reconstructed silicene sheet with a higher Si coverage ratio of 1.17, and, instead, an in-plane compressive strain, we can infer that the observed blend results from a frozen-in dynamic mix occurring at the high growth temperature of $\sim 300^\circ\text{C}$, due to local fluctuations of the Si atom density. Such fluctuations, as suggested by the LEEM studies,^{17,22} would be the consequence of all competing kinetic processes involved: impinging flux, surface diffusion, and partial in-diffusion.

To conclude, we stress that the $2\sqrt{3} \times 2\sqrt{3}R(30^\circ)$ superstructure, per se, out-of equilibrium, is inherently highly defective and inhomogeneous: it is a patchwork of fragmented silicene pieces. Compelling observations and measurements reveal its sudden death, to end, in a dynamic fating process at $\sim 300^\circ\text{C}$, on the one hand, in multilayer islands through a dewetting mechanism, and, on the other hand, in the burial of an alloy, most probably confined below the surface. On the contrary, the well documented $3 \times 3/4 \times 4$ structure formed at $\sim 220^\circ\text{C}$ is a well defined silicene phase.

This work was financially supported within the project “2D-NANOLATTICES” of the Future and Emerging Technologies (FET) program within the 7th framework program for research of the European Commission, under FET Grant No. 270749. C.L. thanks financial support from NSFC (Grant Nos. BC0720024 and BC0720043). G.L.L. warmly thanks financial support by Jiao Tong University. J.F.J. thanks financial support from the National Basic Research Program of China (Grant No. 2013CB921902, 2011CB922202) and NSFC (Grant No. 91021002, 11227404, 91221302). Many fruitful discussions with Professor T. Angot and Dr. E. Salomon are greatly acknowledged.

- ¹ G. G. Guzman-Verri and L. C. Lew Yan Voon, *Phys. Rev. B* **76**, 075131 (2007).
- ² S. Cahangirov, M. Topsakal, E. Aktürk, H. Sahin, and S. Ciraci, *Phys. Rev. Lett.* **102**, 236804 (2009).
- ³ P. Vogt, P. De Padova, C. Quaresima, J. Avila, E. Frantzeskakis, M. C. Asensio, A. Resta, B. Ealet, and G. Le Lay, *Phys. Rev. Lett.* **108**, 155501 (2012).
- ⁴ C.-L. Lin, R. Arafune, K. Kawahara, N. Tsukahara, E. Minamitani, Y. Kim, N. Takagi, and M. Kawai, *Appl. Phys. Express* **5**, 045802 (2012).
- ⁵ A. Fleurence, R. Friedlein, T. Osaki, H. Kawai, Y. Wang, and Y. Yamada-Takamura, *Phys. Rev. Lett.* **108**, 245501 (2012).
- ⁶ Z.-L. Liu, M.-X. Wang, J.-P. Xu, J.-F. Ge, G. Le Lay, P. Vogt, D. Qian, C.-L. Gao, C. Liu, and J.-F. Jia, *New J. Phys.* **16**, 075006 (2014).
- ⁷ Y. Fukaya, I. Mochizuki, M. Maekawa, K. Wada, T. Hyodo, I. Matsuda, and A. Kawasuso, *Phys. Rev. B* **88**, 205413 (2013).
- ⁸ R. Arafune, C.-L. Lin, K. Kawahara, N. Tsukahara, E. Minamitani, Y. Kim, N. Takagi, and M. Kawai, *Surf. Sci.* **608**, 297 (2013).
- ⁹ H. Liu, J. Gao, and J. Zhao, *J. Phys.: Conf. Ser.* **491**, 012007 (2014).
- ¹⁰ A. Resta, T. Leoni, C. Barth, A. Ranguis, C. Becker, T. Bruhn, P. Vogt, and G. Le Lay, *Sci. Rep.* **3**, 2399 (2013).
- ¹¹ N. W. Johnson, P. Vogt, A. Resta, P. De Padova, I. Perez, D. Muir, E. Z. Kurmaev, G. Le Lay, and A. Moewes, *Adv. Funct. Mater.* **24**, 5253 (2014).
- ¹² H. Enriquez, S. Vizzini, A. Kara, B. Lalmi, and H. Oughaddou, *J. Phys.: Condens. Matter* **24**, 314211 (2012).
- ¹³ H. Jamgotchian, Y. Colignon, N. Hamzaoui, B. Ealet, J.-Y. Hoarau, B. Aufray, and J.-P. Bibérian, *J. Phys.: Condens. Matter* **24**, 172001 (2012).
- ¹⁴ H. Jamgotchian, Y. Colignon, B. Ealet, B. Parditka, J.-Y. Hoarau, C. Girardeaux, B. Aufray, and J.-P. Bibérian, *J. Phys.: Conf. Ser.* **491**, 012001 (2014).
- ¹⁵ E. Cinquanta, E. Scalise, D. Chiappe, C. Grazianetti, B. van den Broek, M. Houssa, M. Fanciulli, and A. Molle, *J. Phys. Chem. C* **117**, 16719 (2013).
- ¹⁶ Z.-X. Guo, S. Furuya, J.-I. Iwata, and A. Oshiyama, *Phys. Rev. B* **87**, 235435 (2013).
- ¹⁷ P. Moras, T. O. Montes, P. M. Sheverdyaeva, A. Locatelli, and C. Carbone, *J. Phys.: Condens. Matter* **26**, 185001 (2014).
- ¹⁸ B. Lalmi, H. Oughaddou, H. Enriquez, A. Kara, S. Vizzini, B. Ealet, and B. Aufray, *Appl. Phys. Lett.* **97**, 223109 (2010).
- ¹⁹ H. Enriquez, A. Kara, A. J. Mayne, G. Dujardin, H. Jamgotchian, B. Aufray, and H. Oughaddou, *J. Phys.: Conf. Ser.* **491**, 012004 (2014).
- ²⁰ G. Le Lay, P. De Padova, A. Resta, T. Bruhn, and P. Vogt, *J. Phys. D: Appl. Phys.* **45**, 392001 (2012).
- ²¹ G. Le Lay, S. Cahangirov, L. Xian, and A. Rubio, “Germanene: a novel two-dimensional germanium allotrope akin to graphene and silicene,” *New J. Phys.* (in press).
- ²² A. Acun, B. Poelsema, H. J. W. Zandvliet, and R. van Gastel, *Appl. Phys. Lett.* **103**, 263119 (2013).
- ²³ N. Tsuboi, H. Okuyama, and T. Aruga, *Phys. Rev. B* **71**, 195414 (2005).